DEVELOPMENT OF A HIGH POWER PNEUMATIC SERVO-POSITIONING SYSTEM FOR SPEED GOVERNORS OF HYDRAULIC TURBINES

Yesid Ernesto Asaff Mendoza, yasaff@hotmail.com
Victor Juliano De Negri, victor@emc.ufsc.br
Federal University of Santa Catarina
Department of Mechanical Engineering - LASHIP - Laboratory of Hydraulic and Pneumatic Systems
Campus Universitário - Zip Code: 88040-900 - Florianópolis - SC – Brazil Phone: (++55) 48 3721 7714

Abstract. *This paper presents the theoretical-experimental study of a servo-pneumatic system whose purpose is to control the position of turbine blades used in small hydroelectric power plants (SHPP). The system is composed of two double-acting cylinders controlled through a servo-pneumatic valve with a position sensor and digital controller. The system is designed to meet the requirements of a 400 KW generating group, comparing its performance with commonly used hydraulic systems. A non-linear model was developed for a pneumatic servo-position, which includes non-linear relationship between the mass flow in the servo-valve and the pressure and electric voltage. The actuator is modeled considering the continuity equations in the chambers and the movement equation involving a variable viscous friction model. Based on the developed model, the controller is designed so as to overcome the dynamic limitation and system non-linearity. To validate the mathematic model proposed and the controller, a comparison was made using experimental data from a test bench that provides results with numerical simulations that reproduce experimental conditions. Regarding the characteristics found through generating and testing the mathematical model, fully satisfactory results were achieved, with good agreement between the theoretical results and the actual physically measured data, demonstrating that this model is suitable to verify the performance of pneumatic systems in closed-loop control. These experimental results attest to the efficacy of the servo-pneumatic system in driving speed governors for turbines of small hydroelectric power plants, since a good system response was observed with reference to settling time, position errors and synchronization.*

Keywords*: Pneumatic Servo-Systems, Speed Governors of Turbines, Electric Energy Generation.*

1. INTRODUCTION

Historically, hydraulic systems have been used in speed governors of hydroelectric power plants, where it is necessary to have position control of parts, such as, wicket gates and runner blades in reaction turbines and needles and deflectors in action turbines. However, observing the force levels, settling times and position errors required for the regulation of speed in small hydroelectric power plant, one identifies that this is a domain where pneumatic systems can also be applied.

Pneumatic positioning systems, or servo-pneumatic systems, are not yet intensively used in industry since it is easier to start up and obtain a good control with electric devices, such as, step motors and servo-motors. However, the development of new control techniques and industrial components (sensors, high performance servo-valves, new cylinders and types of seals) have improved the capacity of the pneumatic positioning systems, to a level which competes with electric and hydraulic systems in terms of both cost and performance.

The motivation in substituting the hydraulic drives for pneumatic ones in small hydroelectric power plants is based on several aspects, including: (1) Equipment cost reduction, since pneumatic systems are cheaper than electric and hydraulic ones; (2) Attainment of lightweight systems through a low force/weight ratio of pneumatic components; (3) Use of fewer system components (consequently with more simplified discrete control (automation)) since pneumatic systems do not need a hydraulic power unit to be controlled; (4) Mineral oil not used for power transmission, reducing the environmental risks and the maintenance costs; and (5) Capacity to store energy in a simple way (through air reservoirs) to carry out emergency operations. Based on these aspects, this paper presents the study of a pneumatic servo-system developed to control the position of wicket gates on a 400 kW Francis Turbine, where loads about 12,000N are overcome and the static and dynamic requirements are reached.

Regarding the structure of the paper, in section 2.0 the specifications of the servo-pneumatic system and its sizing are defined, in section 3.0 the mathematical modeling is presented. The test rig is described in section 4.0, the theoretic-experimental results are given in the section 5.0 and in the section 6.0 the conclusions are presented.

2. THE PNEUMATIC SERVO-SYSTEM

The design requirements were defined for the system considering the static and dynamic behavior needed for Small Hydroelectric Power Plants (SHPP). The general specifications of speed governors that need to be attended are given by standards ANSI/IEEE 125 (IEEE, 1988) and IEC 61262 (IEC, 1997) and, for the specific case of small power plants,

the specifications supplied by the company Reivax Automação e Controle and the previous results from research projects executed at the Laboratory of Hydraulic and Pneumatic Systems – LASHIP were also considered.

According to the IEC 61362 standard (IEC, 1997), the time constant of the servo-positioner that controls the wicket gate opening must be between 0.1s and 0.25s, which was considered as a requirement for the pneumatic positioning system under analysis. At the same time, the maximum positioning error of the servo-system was established as 1% of the total stroke. Taking into account technical data from several SHPP installed in Brazil, a generating group composed of a Francis turbine with a power of 400kW and a drop height of 50m was chosen for this study.

The servo-motor (cylinder) opening/closing times were defined as 5s. As established at IEC 61362 (IEC, 1997), the servo-motor opening/closing speeds must be adjustable independently, through specific devices, in such way that these maximum speeds avoid turbine over speed and water hammer.

The speed-governor manufacturer normally defines the stroke of the servo-motor. However, it can be seen that the range of strokes is between 115mm to 200mm for SHPPs. A stroke of 160mm was used to allow a maximum force of 12,000N considering the power and drop height conditions presented above (Asaff, 2006). As a consequence, for the movement of the gate operating ring an actuating pneumatic circuit was adopted, composed by two single-rod double-acting cylinders of 125mm piston diameter and 32mm rod diameter, as shown in Figure 1. The cylinders are controlled through a pneumatic servo-valve with 700NL/min nominal flow rate, in order to guarantee the maximal force in all opening/closing speed situations.

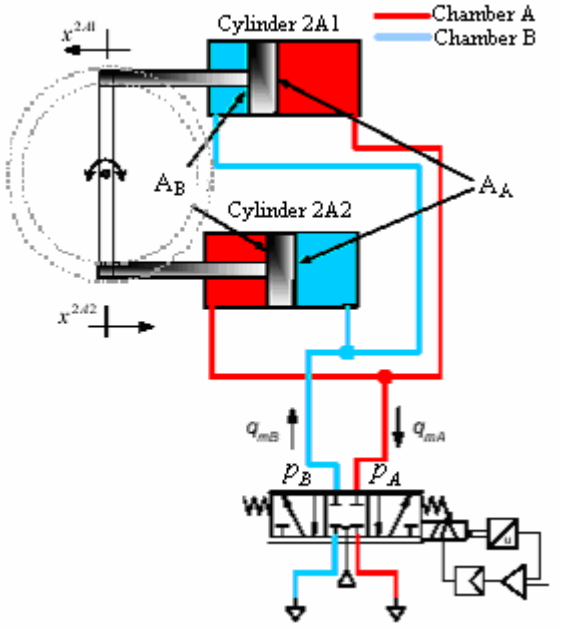

Figure 1. Pneumatic circuit for speed-governing

3. MATHEMATICAL MODELING

As presented in Scholz (1990) and Vieira (1998), the mass flow rate through the valve is modeled according to the ISO 6358 standard (ISO, 1989), which describes the state of the subsonic flow through an elliptic curve which is dependent on the parameters b (saturation point) and C (sonic conductance). Therefore, the mass flow rate is described by Eqs. (1) and (2), which are valid for the subsonic ($a > b$) and sonic ($a \leq b$) conditions, the latter including the saturated flow that occurs when the pressure rate is lower than the critical pressure rate.

$$q_m = A_{re} C p_1 \rho_o \sqrt{\frac{T_o}{T_1}} w(a) \tag{1}$$

$$w(a) \begin{cases} = \sqrt{1 - \dfrac{(a-b)^2}{(1-b)^2}} & \text{for} \quad a > b \\ = 1 & \text{for} \quad a \leq b \end{cases} \tag{2}$$

Where, a=(p_2/p_1) and b=$(p_2/p_1)_{cr}$=0.528, p_1 and p_2 are the absolute pressures at the upstream and downstream of the orifice, respectively. T_1 is the upstream temperature, T_0 *is* the temperature at the NTP[1], ρ_o is the density at NTP, A_{re} is the relative opening of the servo-valve and C is the sonic conductance equal to 0.3 according to the catalogue of the valve.

The servo-valve opening is calculated by the variable called "relative opening (A_{re})" adopted in Vieira (1998), which takes into account the dead-zone, the asymmetry and the flow saturation of the servo-valve. The relative opening is determined experimentally through a process of pressurizing and depressurizing of known chamber volumes connected to ports A and B of the servo-valve. Applying the continuity equation, it is possible to calculate the mass flow rate based on the pressure variation in these chambers.

The relative opening curves for ports A (P→A and A→T) and B (P→B and B→T) for the servo-valve used are shown in Fig. 2(a). The equations that represent these curves are obtained by the polynomial method described in Vieira (1998), which establishes the relation between the input voltage (U) and the relative opening (A_{re}).

The servo-valve has a region where there is no flow with non-zero input voltage, as can be seen in Fig. 2. As demonstrated in Valdiero (2004), the dead-zone (ZM) can be compensated for in the closed-loop system by including a function before the servo-valve that computes the inverse of the ZM but is linearly smoothed at the origin. Figure 2 (b) shows the ZM inverse, where u_d is the required input voltage in the absence of ZM, u_{czm} is the compensator signal and lc is the compensation width that defines the region of linear smoothing. This compensation is described by Eq. (3). The following values can be assumed for the servo-valve used here: $md = me = 1$, $zmd = 0.61$V, $zme = 0.69$V and $lc = 0.4$.

$$u_{czm}(t) = \begin{cases} \dfrac{u_d(t)}{md} + zmd & se \quad u_d(t) \geq lc \\ \dfrac{u_d(t)}{me} - |zme| & se \quad u_d(t) \leq -|lc| \\ \left(\dfrac{zmd + lc/md}{lc} \right) u_d(t) & se \quad 0 \leq u_d(t) < lc \\ \left(\dfrac{|zme| + |lc|/me}{|lc|} \right) u_d(t) & se \quad -|lc| \leq u_d(t) < 0 \end{cases} \tag{3}$$

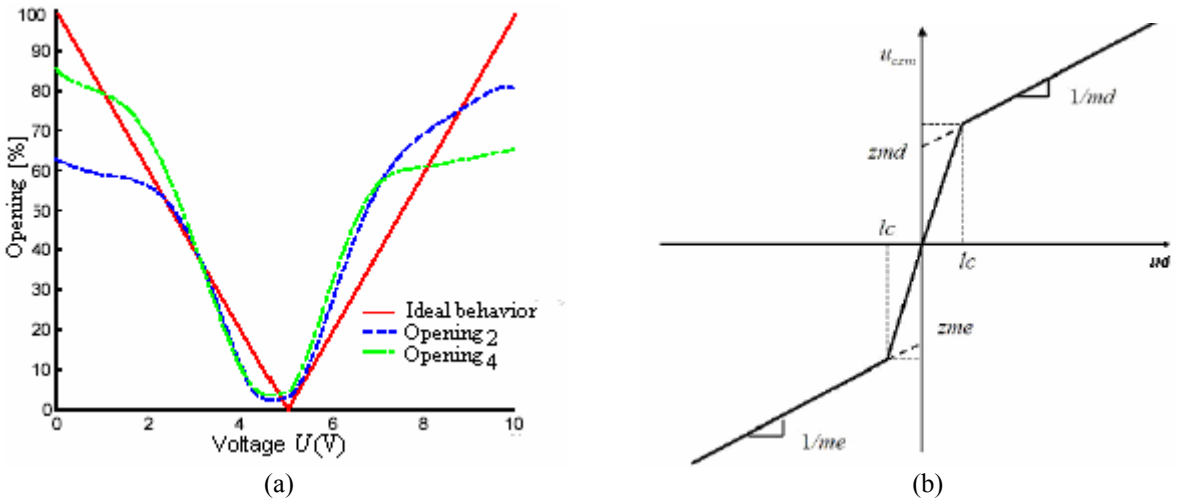

(a) (b)

Figure 2. Servo-valve characteristics. (a) Relative opening curves (Vieira, 1998) (b) Graphical representation of the inverse of the dead-zone non linearity (Valdiero, 2004)

[1] NTP: Normal Temperature and Pressure: p=1.013x10^{5}Pa (1.013bar), T=20°C (293.15K), ρ=1.204 kg/m^3.

For the cylinders, Barreto (2003) and Perondi (2002) describe the dynamic behavior of the air in the chambers through the conservation of mass or energy laws, as considered by Karpenko and Sepehri (2004). The hypothesis of isentropic flow and no internal or external leakage of the chambers are considered.

Considering the pneumatic circuit shown in Fig. 1, where two cylinders are connected to the same valve, the volume V_A is calculated with the addition of the volumes of the cylinder A chambers; the position $x^{2A1}=0$ is attained when cylinder 2A1 is retracted and position $x^{2A2}=0$ when cylinder 2A2 is in the advanced position. Equation (4) describes the pressure variation in the A chambers of cylinders 2A1 and 2A2

$$\frac{dp_A}{dt} = -\frac{v\gamma\left(A_A^{2A1} + A_B^{2A2}\right)}{V_{A0}^{2A1} + A_A^{2A1}x^{2A1} + V_{A0}^{2A2} + A_B^{2A2}x^{2A2}}p_A + \frac{RT_A\gamma}{\left(V_{A0}^{2A1} + A_A^{2A1}x^{2A1} + V_{A0}^{2A2} + A_B^{2A2}x^{2A2}\right)}q_{mA} \tag{4}$$

where "q_{mA}" is the mass flow rate from the servo-valve to chamber A, "V_{A0}" is the dead volume in chamber A including the pipelines as being equal to $98.17\text{x}10^{-5}\text{m}^3$; "$T_A$" is the absolute temperature in chamber A, "R" is the gas constant equivalent to 287 J/kg.K, "A_A" and "A_B" are the piston areas, x is the displacement of the cylinders 2A1 and 2A2; "γ" is the specific heat ratio at constant pressure and constant volume.

Likewise, the continuity equation for the B chambers of the cylinders can be written in the following form:

$$\frac{dp_B}{dt} = \frac{v\gamma\left(A_B^{2A1} + A_A^{2A2}\right)}{V_{B0}^{2A1} + A_B^{2A1}\left(L - x^{2A1}\right) + V_{B0}^{2A1} + A_A^{2A2}\left(L - x^{2A1}\right)}p_B - \frac{RT_B\gamma}{\left(V_{B0}^{2A1} + A_B^{2A1}\left(L - x^{2A2}\right) + V_{B0}^{2A2} + A_A^{2A2}\left(L - x^{2A2}\right)\right)}q_{mB} \tag{5}$$

where: "q_{mB}" is the mass flow rate from the servo-valve to chamber B, "L" is the cylinder stroke and "V_{B0}" is the dead volume in chamber B including the pipelines as being equal to $98.17\text{x}10^{-5}\text{m}^3$; "$T_B$" is the absolute temperature in B chamber and "γ" is the specific heat ratio at constant pressure and constant volume.

The equilibrium forces in the pistons are obtained by the application or Newton's Second Law. Considering that in the cylinders the rod extremities are connected and neglecting the rod angle variation in relation to the interconnection lever, results in:

$$p_A A_A^{2A1} - p_B A_B^{2A1} + \left(-p_A A_B^{2A2} + p_B A_A^{2A2}\right) - F_{a1} - F_{a2} - Fc = M\frac{d^2x^{2A1}}{dt} \tag{6}$$

where "M" is the total mass that equals 30 kg, "F_C" is the load force, and "Fa_1" and "Fa_2" are the friction forces between the pistons and the sleeve of each cylinder, respectively.

For the representation of the friction compensation the model of the variable viscous friction coefficient presented by Gomes and Rosa (2003), and optimized by Machado (2003), is adopted in this study. This model represents the "stick" and "slip" modes through different trajectories in the "stick-slip" region. It is worth noting that, in practice, the velocities are considered close to zero when they are smaller than the speed limit, below which it is not possible to displace the body with constant speed. In the variable viscous friction coefficient model, the friction force for speeds above the speed limit is obtained from the friction-velocity maps, which define the relation between the friction force and the relative velocity between the contact surfaces.

The experimental results for the cylinders are shown in Fig. 3, using friction-velocity maps, from which the Coulomb friction parameters, variable viscous friction coefficient, limit speed and static friction can be extracted. These parameters are then used together with the "stick" speed in the implementation of the representative friction model. These maps are constructed by measuring the force applied to achieve a movement of constant speed, without external load being applied to the cylinder. In the model presented in Asaff (2006), the friction force is described by:

$$F_{ai} = f_{Vi}\dot{x}_i \tag{7}$$

where "$\dot{x}_i$" is the speed displacement at the operation point "i" and "f_{Vi}" is the variable viscous friction coefficient, which is a function of the velocity "$\dot{x}_i$" and the applied force.

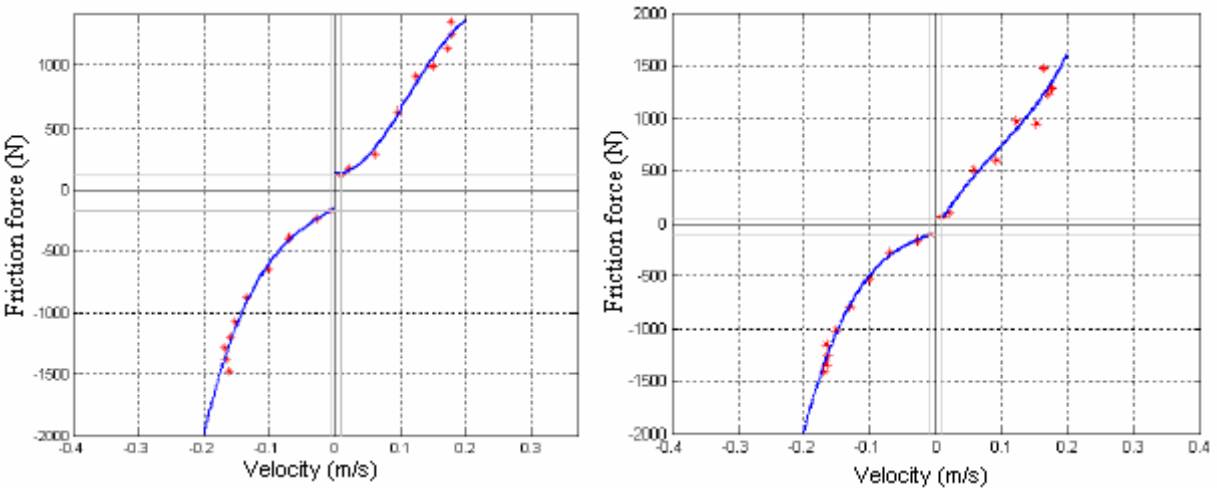

Figure 3. Friction-velocity maps. (a) Cylinder 2A1. (b) Cylinder 2A2

Finally, the control signal generated by the PID controller can be generically express by Eq. (8). In the simulations and tests, the implementation of the controller was carried out using MATLAB/SIMULINK, in which the mathematical model was represented in blocks diagrams, as shown in Fig. 4.

$$u_d(t) = Kp(e(t) + \frac{1}{Ti}\int_0^t e(\tau)d\tau + T_d\frac{de(t)}{dt} \tag{8}$$

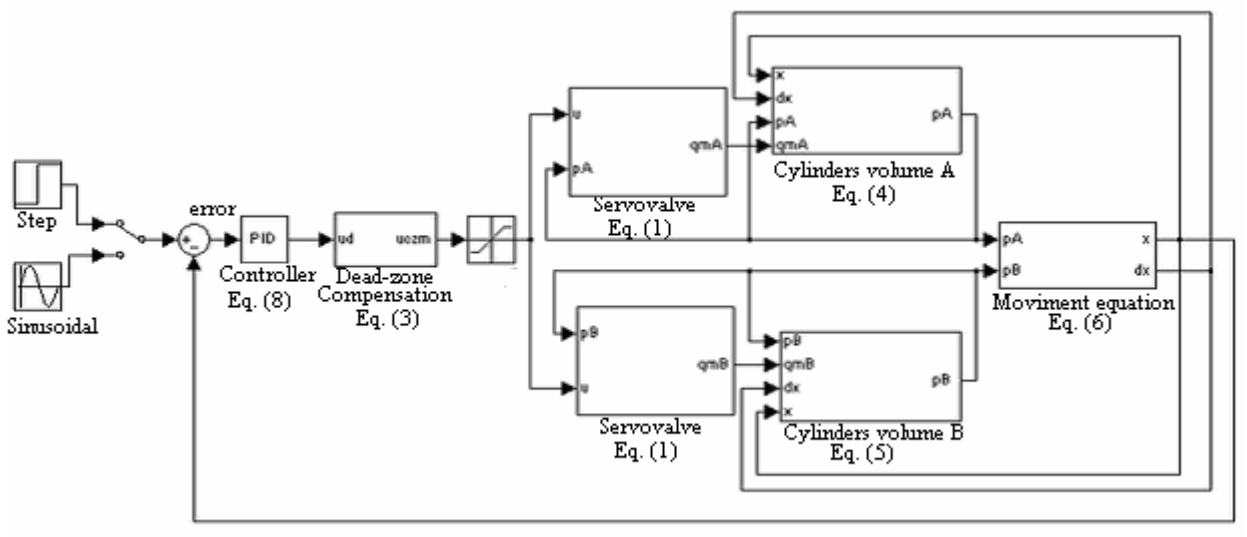

Figure 4. Representation of the mathematical model of the system in block diagrams.

4. TEST RIG

The experimental implementation of the system was carried out using the test rig shown in Fig. 5, at the Laboratory of Hydraulic and Pneumatic Systems (LASHIP), Department of Mechanical Engineering, Federal University of Santa Catarina. In the test rig, the components are arranged according to the schematic representation of the servo-pneumatic system shown in Fig. 6, including an ultrasonic position transducer connected to one of the two double-acting cylinders and one 5-port servo-valve, that put simultaneously in motion the two cylinders from a signal originated in the controller. The pressure proportional valve, together with the air reservoir, has the function of keeping a constant air supply pressure for the servo-valve.

The system that generates the load force is constituted by a hydraulic circuit, which is composed of a double-acting, single-rod, hydraulic cylinder commanded by a directional valve, a pressure regulation valve and a power unit. Thus,

the system that emulates the mechanical work required in the gate ring is formed by a lever pivoted at its center and connected at its extremities to the pneumatic cylinders and load hydraulic cylinder. The acquisition and control system used was a dSPACE board, composed of four analog inputs (ADCs) and four analog outputs (DACs), installed in a desk top computer.

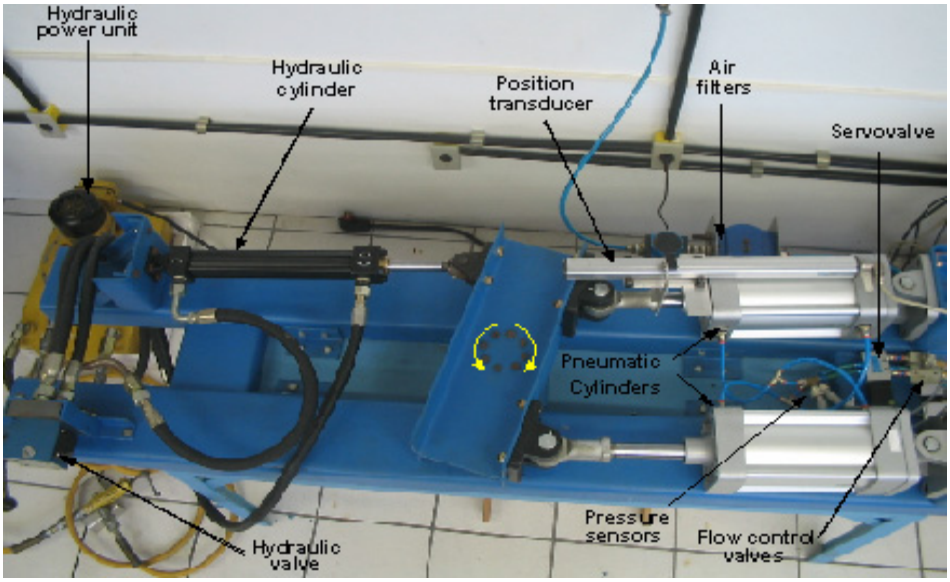

Figure 5. The test rig

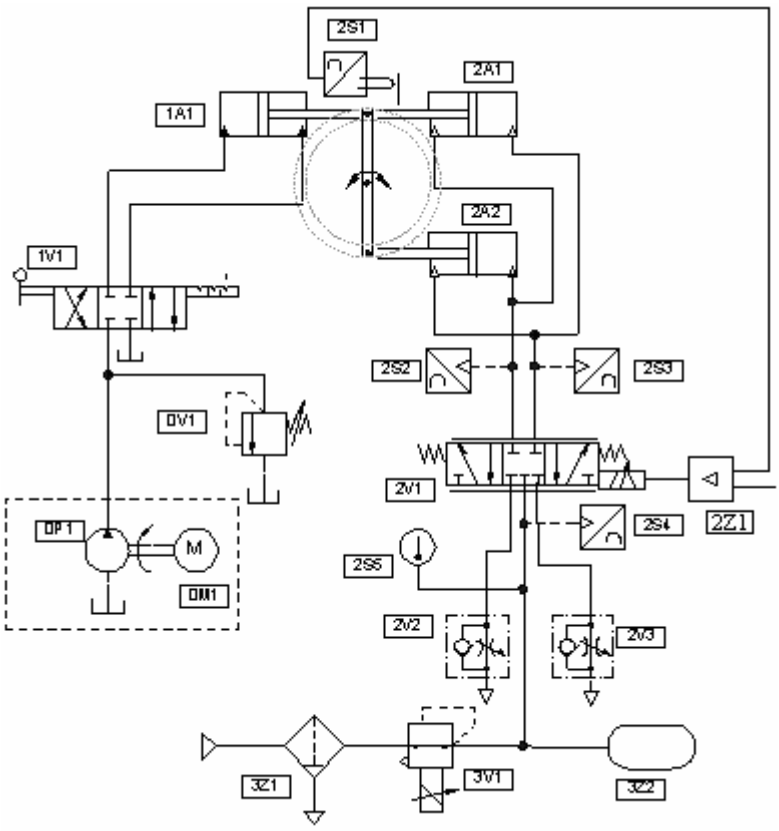

Figure 6. Circuit diagram of servo-pneumatic system (codification according to Table 1)

Table 1. Components of the experimental test rig.

COMPONENT CODES			
Component	**Code**	**Component**	**Code**
Hydraulic pump	0P1	Ultrasonic position transducer	2S1
Electric motor	0M1	Absolute pressure transducer	2S2, 2S3
Hydraulic pressure regulation valve	0V1	Differential pressure transducer	2S4
Directional control valve of 4-port	1V1	Type J thermocouple	2S5
Hydraulic cylinder	1A1	Pneumatic cylinder	2A1, 2A2
Pneumatic servo-valve 5-port	2V1	PID controller	2Z1
Flow control valve	2V2, 2V3	Air filter unit	3Z1
Proportional pressure regulation valve	3V1	Air receiver	3Z2

5. RESULTS

The results obtained using the test rig are presented in this section. In general, they validate the high power servo-pneumatic system developed for specific application in turbine speed governors of small hydroelectric power plants. The tests were carried out in the test rig described in section 3.0, where the responses to sinusoidal and step input signals of the servo-system were measured.

In order to analyze the system under different operational conditions, the initial position of the cylinders and the load force were varied, considering a nominal load force of F_{Cn}=12,000N. For the input signal of the system, the four values for the reference amplitude of the signal step were established: 1%, 2%, 5% and 10% of the cylinder stroke (L = 160mm). Also, tests were carried out with a sinusoidal trajectory in the form of $xd(t)= xsen(\omega t)$, where x = 8mm (5% of the cylinder stroke) $\omega= \pi/10$rad/s (0.05 Hz). As shown in Fig. 7, the operation force required for the drive mechanism of the speed governor distributor ring has a typical behavior as a function of the turbine wicket gate opening.

Hence, tests were performed considering the critical regions (1) and (2) (Fig. 7). The nominal rotation without turbine load occurs with approximately 15 % of the distributor opening. For the nominal power, corresponding to 80 to 90% of the distributor opening, 100% of the F_{Cn} was applied

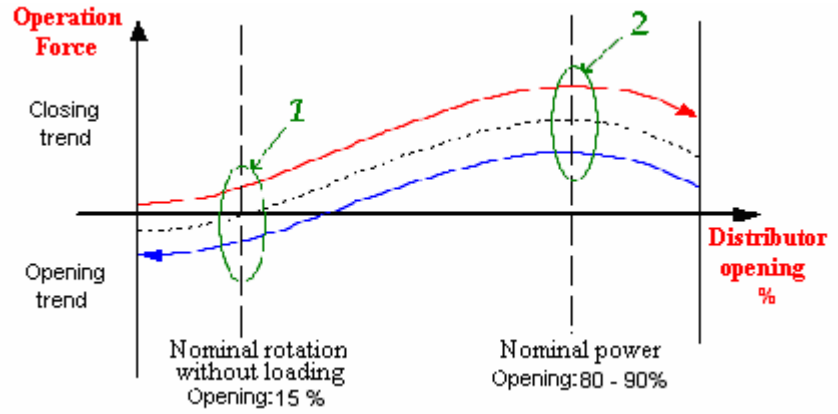

Figure 7. Operation force diagram of the distributor (adapted from Asaff, 2006)

The PID controller gains used were established through studies with the mathematical model as well as the test rig, aiming to obtain limits for which the control signals and the responses still present smooth behaviors. All the measured signals (supply pressure, cylinder chamber pressure and cylinder position) were filtered through first-class low-pass filters to reduce the electromagnetic interference from the environment and also to obtain the velocity from numerical derivation of the displacement. The supply pressure of the system was regulated at 0.8MPa$_{abs}$ (8bar$_{abs}$) and the supply air temperature was monitored, being in the range of 19 to 22°C.

5.1. Theoretical and experimental results

The developed model was validated through the comparison between simulation and experimental data. It is important to emphasize that the parameters of the pneumatic system and the experimental data, including the friction-velocity maps of the cylinders, the servo-valve dead-zone and the equations presented in section 3, allow the complete computational implementation of the model, aiming to extrapolate it to other pneumatic servo-system designs.

Figure 8 allows a comparison between the experimental curves of the position with and without dead-zone compensation, so that the phenomenon can be analyzed in detail. A better performance is obtained when compensation is used, since this strategy eliminates the effect of the valve asymmetry and shifts the voltage that commands the valve to guarantee a flow rate different to zero when necessary, reducing the settling time of the system. In Fig. 9 the theoretical and experimental results with an input step of 2% of the cylinder stroke for F_C=11,400N are presented, with a settling time of ts=1.18s in the steps in 4s and 9s and for a steady state error of 0.32mm. For the step in t=14s the settling time was ts=0.55s.

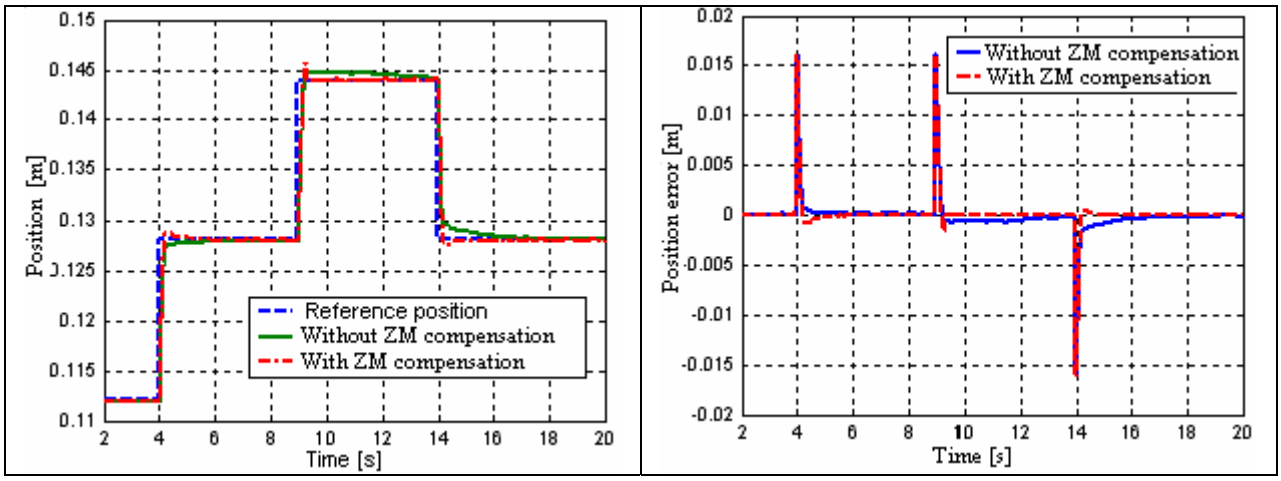

(a) (b)

Figure 8. System response for a step sequence of 10% of stroke with and without dead-zone compensation, without load (PID controller gains (K_P=280, K_I=0.2, K_D=6). (a) Position (b) Position error

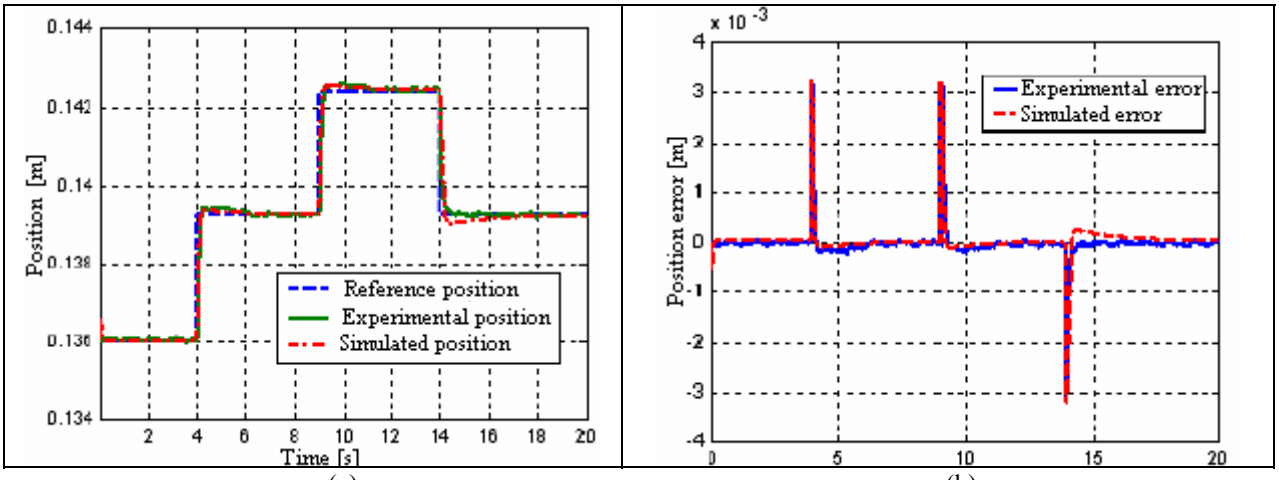

(a) (b)

Figure 9. System response with load, for a step sequence of 2% of cylinder stroke, with initial position of 136mm with ZM compensation (K_P=280, K_I=0.2, K_D=6) (a) Position (b) Position error

5.2. Test results for the speed governor

For the tests related to the application as a speed governor, installation and adjustment of the flow regulating valves (2V2 and 2V3 in Fig. 6) was carried out, to achieve times of t_a=5s and t_f=5s, applying a load of F_C=5,700N (approximately 50% of the F_{Cn}), obtaining a maximum speed close to 0.09m/s. Figures 10, 11 and 12 show the system response for different inputs. In Figure 10, the position system response for a step of 5% of cylinder stroke and a settling time of approximately ts=0.33s, with a steady state error of 0.24mm for the positive step, and ts=0.56s, with a steady state error of 0.24mm for the negative step, is shown.

The critical region (1) shown in Fig. 7 is related to the nominal rotation region in the initial position of 15% of the servo-motor stroke. Normally, this point is designed to be a load zero region, but the action of the distributor control at

this point may have a positive load, closing the distributor, or a negative load, opening the distributor. Figure 11 describes the test for positive load, achieving a settling time in the order of 1.4s with position errors of 0.8mm. In the opposite case, shown in Fig. 12, with negative load, the settling time achieved was 0.5 to 0.6s, with a steady state error of 0.27mm.

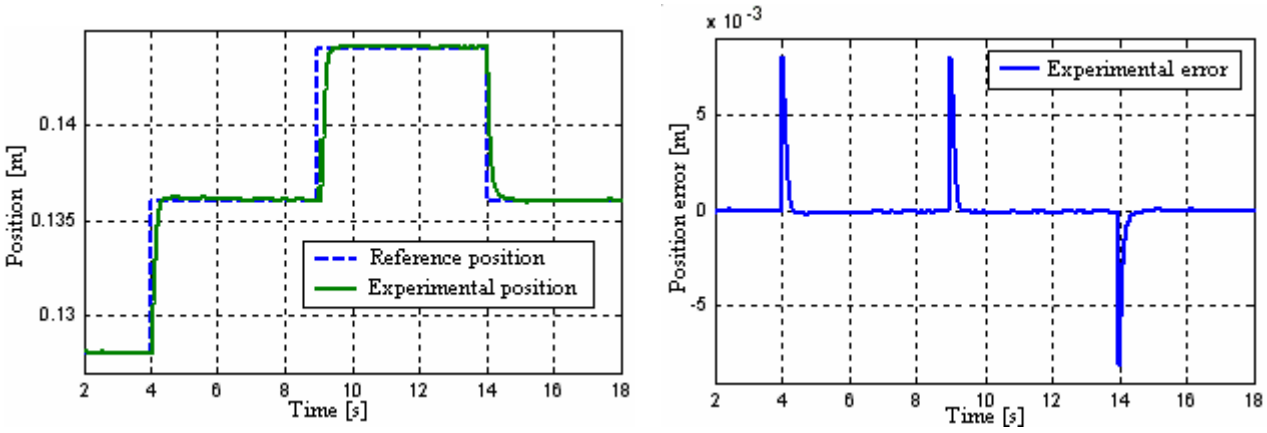

Figure 10. System response with positive load of Fc=11,200N, for a step sequence of 5% of cylinder stroke, with initial piston position of 128mm (K_P=280, K_I=0.2, K_D=20)

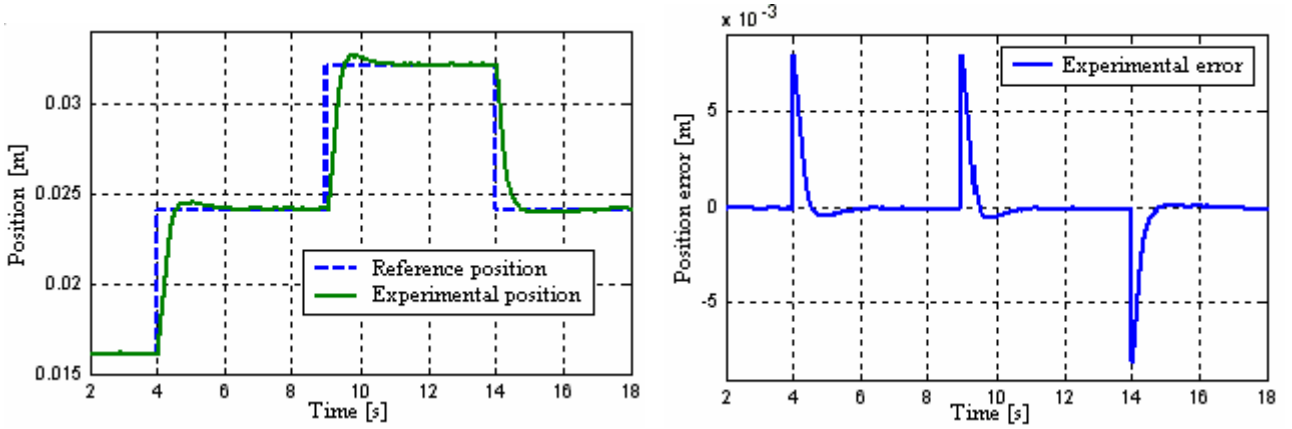

Figure 11. System response with positive load of Fc=2,300N for a step sequence of 5% of cylinder stroke, with initial piston position of 16mm (K_P=280, K_I=0.2, K_D=20)

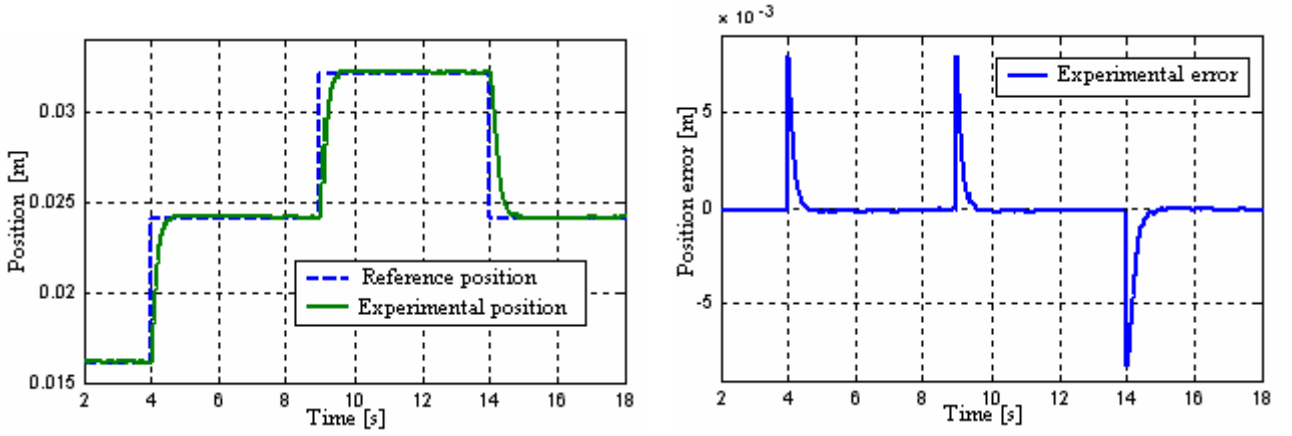

Figure 12. System response with negative load of Fc=2,300N for a steps sequence of 5% of cylinder stroke, with initial piston position of 16mm (K_P=280, K_I=0.2, K_D=20)

6. CONCLUSIONS

Through the experimental implementation, the effectiveness of PID controller with dead-zone compensation of the servo-valve was confirmed, overcoming the non linearity associated with the flow in the valve and reducing the oscillations due to the air compressibility. The theoretical results are in good agreement with the experimental ones, showing the flexibility of the model in relation to describing other servo-pneumatic systems.

The results obtained verify the effectiveness of the servo-pneumatic system for the control of high forces, especially in the control of speed governing of turbines with a PCH of up to 400 kW. It was observed through the tests carried out with different step amplitudes and a sinusoidal signal (1, 2, 5 and 10% of the stroke), that the response system was fully adjusted in relation to the settling times, and the position errors of 0.5 to 0.8% of the total cylinder stroke, were below the 1% required for speed governors. It should be noted that there was a good repeatability identified in all the tests in relation to the static and dynamic specifications reached. Given the equipment existing in the market and the analysis carried out in this study, it is presumed that the pneumatic system can deal with systems with a power of up to 3MW.

7. ACKNOWLEDGEMENTS

The authors are grateful to CNPq for grants and to *Reivax Automação e Controle* for the specifications section and the financial support of the project.

8. REFERENCES

Asaff, Y. E., 2006, “Development of a Servo-pneumatic System for Speed Governors of Turbines in Small Hydroelectric Power Plants”, (In Portuguese), Master’s Thesis, Mechanical Engineering Department, Federal University of Santa Catarina, Brazil

Barreto, F., 2003, “Project of a Industrial Servo-pneumatic Positioning Appling Cascade Control”, (In Portuguese), Master’s Thesis, Mechanical Engineering Department, Federal University of Santa Catarina, Brazil

Gomes , S. C. P.; Rosa, V. S., 2003, A new approach to compensate friction in robotic actuators. In: International Conference On Robotics And Automation, 2003, Taipei, Taiwan. Proceedings... [S.I]: IEEE,.

IEC., 1997, “IEC 61362 - Guide for Specification of Hydroturbine Control Systems”, Switzerland, 105p.

IEEE., 1988, “ANSI/IEEE Std. 125 - Recommended Practice for Preparation of Equipment Specifications for Speed-Governing of Hydraulic Turbines Intended to Drive Electric Generators”, USA, 28p.

ISO International Organization for Standardization, 1989, “ISO 6358 - Pneumatic Fluid Power - Components Using Compressible Fluids,- Determination of Flow Rate Characteristics”, Switzerland, 13 p..

Karpenko, M., Sepehri, N., 2004, “Design and Experimental Evaluation of a Nonlinear Position Controller for a Pneumatic Actuator with Friction”, Proceeding of the 2004 American Control Conference, Boston, pp 50-78.

Lee, H. K., Choi, G. S., Choi, G. H., 2002, “A Study on Tracking Position Control of Pneumatic Actuators”, Mechatronics, Volume 12, Inssue 6, South Korea pp 813-831.

Machado, C., 2003, “Friction Compensation in Hydraulic Actuators used Artificial Neural Network”, (In Portuguese), Master ‘s Thesis, Mechanical Engineering Department, Federal University of Santa Catarina, Brazil

Nouri, B., Ai-Bender, F., Swevers, J., Vanherck, P. e Van Brussel, H., 2000, “Modeling a Pneumatic Servo Positioning System With Friction”, Proceedings of the ACC 2000, pp. 1067-1071.

Perondi, E.A.,2002,"Cascade Nolinear Control with Friction Compensation of a Pneumatic Servo Positioning" (In Portuguese), Doctor Thesis, Mechanical Engineering Department, Federal University of Santa Catarina, Brazil, 178p.

Scholz, Dieter., 1990, “Auslegung Servopneumatischer Antriebssystemse, (In German), PhD Thesis, IHP-RWTH, Aachen, Alemanha.

Valdiero, A., 2004, “Control of Hydraulic Robots with Friction Compensation”, (In Portuguese), Doctor Thesis, Mechanical Engineering Department, Federal University of Santa Catarina, Brazil, 188 p.

Vieira, A. D., 1998, “Theoretical and Experimental Analysis of Pneumatic Linear Position Servo Systems” (In Portuguese), Master’s Thesis, Mechanical Engineering Department, Federal University of Santa Catarina, Brazil.

Zorlu, A., Ozsoy, C., and Kuzucu, A., 2003, “Experimental Modeling of a Pneumatic Emerging Technologies and Factory Automation, Proceedings. ETFA '03, IEEE Conference, pp 453.

9. RESPONSIBILITY NOTICE

The authors are the only people responsible for the printed material included in this paper.